# Electrostimulated Release of Neutral Drugs from Polythiophene Nanoparticles: Smart Regulation of Drug-Polymer Interactions

**Anna Puiggalí-Jou, Paolo Micheletti, Francesc Estrany, Luis J. del Valle* and Carlos Alemán***

**Mrs. A. Puiggalí-Jou, Mr. P. Micheletti, Dr. F. Estrany, Dr. L. J. del Valle and Prof. Dr. Carlos Alemán.** Departament d'Enginyeria Química (EEBE) and Barcelona Research Center for Multiscale Science and Engineering, Universitat Politècnica de Catalunya, C/ Eduard Maristany, 10-14, Ed. I2, 08019, Barcelona, Spain. Correspondence to: luis.javier.del.valle@upc.edu and carlos.aleman@upc.edu

## ABSTRACT

Poly(3,4-ethylenedioxythiophene) (PEDOT) nanoparticles have been loaded with curcumin and piperine by *in situ* emulsion polymerization using dodecyl benzene sulfonic acid (DBSA) as both stabilizer and doping agent. The loaded drugs affect the morphology, size and colloidal stability of the nanoparticles. Furthermore, kinetics studies of non-stimulated drug release have evidenced that polymer···drug interactions are stronger for curcumin than for piperine. This observation suggests that drug delivery systems based on combination of the former drug with PEDOT are very appropriated to show an externally tailored release profile. This has been demonstrated by comparing the release profiles obtained in presence and absence of electrical stimulus. Results indicate that controlled and time-programmed release of curcumin is achieved in a physiological medium by applying a negative voltage of –1.25 V to loaded PEDOT nanoparticles.

**Keywords:** Anticancer Agent; Conducting polymer; Curcumine; Controlled release; Piperine

## 1. Introduction

Electroactive conducting polymers (ECPs) allow excellent control of the electrical stimulus, possess very good electrical and optical properties, have a high conductivity/weight ratio and can be biocompatible, biodegradable and porous.[1] Furthermore, a great advantage of ECPs is that their properties can be tailored to the specific needs of their applications by incorporation of biopolymers, peptides, or other bio-related moieties.[2]

On the other hand, on-demand release of drug molecules from biomedical devices enables precise targeted dosing that can be temporally tuned to meet requirements for a variety of biomedical applications.[3,4] Recent advances have facilitated the use of different stimuli, such as light, magnetic and electric fields, ultrasounds and electrochemical signals, to trigger drug release from smart material formulations (*e.g.* films, micro- and nanoparticles, and implant devices).[4,5] These technologies enable greater control over drug delivery compared to traditional systems that cannot be modified in response to changing therapeutic needs (*e.g.* systems based on biodegradability of polymers).

Electro-responsive drug-delivery systems are particularly attractive in this regard because electrical signals can be generated relatively easily, be accurately controlled and be remotely applied without using large, specialized and complex equipment. Moreover, it is possible to develop drug-delivery systems that allow repetitive dosing. In particular, recent in vivo assays have proved that ECPs nanoparticles (NPs) are successful electro-responsive drug delivery systems.[6,7] Thus, the application of a small external electric field to these systems, which were subcutaneously localized by syringe injection at the place of interest, released the drug from the NPs, allowing its diffusion to the surroundings.

At present time, the existence of multiple methods to incorporate drugs into ECP matrices for their subsequent release indicates that these organic materials are potential platforms for controlled drug delivery.[8] For example, molecules bound in ECPs films[9] through doping can be controllably expelled by applying a reducing electrical potential. Thus, the fact that they can be made porous and have delocalized charge carriers aids in the diffusion of the bound molecules, adding a further reason why ECPs are very suitable for drug release applications.[10] Nevertheless, formulations based on ECPs thin films, which are the most frequent ones, present low drug loading as a major disadvantage.[11] Although more drug can be incorporated by increasing the thickness of the films, the majority of the release takes place at the surface while drug molecules at the bulk remain. Compared to films, ECP NPs have increased surface-to-volume ratio,[12] allowing higher drug loading. In spite of their small size, ECP NPs are electrically and electrochemically responsive, which is expected to be very advantageous for the design of controllable and programmable drug delivery systems. Considering the vast amount of possibilities, ECP NPs will undoubtedly play a decisive role in all disciplines of sciences that require programmed delivery of chemical compounds, including the biomedical field.

In some recent but still scarce studies, NPs of polypyrrole (PPy), which is probably the most studied non-toxic ECP,[13] has been used to trigger sensitive dosage-controlled release of drugs.[6,14,15] More specifically, the response of PPy NPs embedded in a hydrogel against a dual stimulus (temperature and electric field) was demonstrated through in vivo experiments.[6] Additionally, the on demand release of drugs with different polarities and molecular weights from electroresponsive PPy NPs has been evaluated.[14] The biocompatibility and linear response achieved with a repetitive and pulsed release evidenced that such approaches are facile and minimally invasive for

potential medical applications.[6,14] Besides, the pH-sensitive behavior of drug loaded PPy NPs has been also reported,[15] reflecting that the release can be controlled through the pH, the charge of the drug and/or the addition of charged amphiphiles.

Among ECPs, poly(3,4-ethylenedioxythiophene) is probably the most employed for the fabrication of biomedical devices because of its outstanding capacitive performance, fast doping-undoping process, stable charge-discharge response, and high conductivity, biocompatibility and stability in continuous operation.[16-18] The structure, surface morphology and porosity of PEDOT and the above discussed PPy are completely different[17,19] since the former is exclusively formed by $\alpha,\alpha$-linkages while the latter is highly crosslinked. Consequently, both the electrochemical and electrical responses of PEDOT are greatly superior to those of PPy. In spite of these advantages, the loading of drugs into PEDOT NPs for release on demand remains practically unstudied. Paradee and Sirivat[20] examined the electrically-controlled release of benzoic acid loaded on PEDOT NPs blended with alginate hydrogels. More recently, Liu *et al.*[21] loaded 2-phenylethynesulfonamide, which is a heat shock protein 70 (HSP70) inhibitor, into thermo-responsive poly(*N*-isopropylacrylamide) shells, incorporating PEDOT NPs as photothermal coupling agent.

In this work two neutral and hydrophobic drugs have been loaded into PEDOT NPs (drug/PEDOT NPs) during their synthesis by emulsion polymerization in water. These drugs are curcumin (CUR), which displays a wide spectrum of medical properties ranging from anti-bacterial, anti-viral, anti-protozoal, anti-fungal, and anti-inflammatory to anti-cancer activity,[22] and piperine (PIP), a piperidine alkaloid with pharmacological properties as anti-inflammatory, antifertility and stimulator of serotonin synthesis in the central nervous system, among others.[23] The release of the drugs from the ECP NPs has been investigated without and with electrostimulation. Results have demonstrated

that PEDOT NPs loaded with CUR serve as a drug reservoir for electric-field triggered release.

## 2. Results and discussion

Although different approaches have been proposed to synthesize ECP NPs from their corresponding monomers combined with soft-templates,[24] they have been criticized because of the poor control on both size and colloidal stability. Moreover, the difficulty of getting rid of the surfactant is added.[25] In a recent study, Zhou and coworkers prepared PEDOT NPs with a particle size distribution of 17.2±1.6 nm applying a hydrothermal approach and using $FeCl_3 \cdot 6H_2O$ as oxidant and sodium dodecyl benzene sulfonate as stabilizer.[26] In the present study, PEDOT NPs have been obtained in water at 40 ºC using dodecyl benzene sulfonic acid (DBSA) as stabilizer and doping agent simultaneously, and ammonium persulfate (APS) as oxidizing agent (Figure 1b). It is worth noting that the stabilizer is required to avoid the yielding of the ECP as an insoluble bulk powder with very limited processability.[27] The effective diameter ($D_{eff}$) of the resulting PEDOT NPs, which are displayed in Figure S1, was 35±6 and 84±2 nm, as determined by scanning electron microscopy (SEM) and dynamic light scattering (DLS), respectively.

The two drugs, CUR and PIP (Figure 1c), considered in this work were loaded *in situ* during the emulsion polymerization. Due to their hydrophobicity, the drugs remained into the cores of the surfactant micelles rather than interacting with the medium. After polymerization, PEDOT NPs were formed and drugs were successfully loaded. The drug loading ratio (DLR), which was expressed as mass of encapsulated drug with respect to the total mass, was 5.9±1.6% and 8.0±0.4% for CUR and PIP, respectively, these values being similar to those achieved using other polymeric vesicles.[28]

Moreover, the successful loading of the drugs within the PEDOT NPs was further confirmed by FTIR spectroscopy, discussed afterwards.

CUR- and PIP-loaded PEDOT NPs, hereafter denoted as CUR/PEDOT and PIP/PEDOT NPs, respectively, are spherical and stable in solution (Figure 2). Despite the CUR and PIP are neutral, hydrophobic and of similar size (*i.e.* 368.4 g/mol and 285.3 g/mol, respectively), the average effective diameter ($D_{eff}$) of loaded NPs was found to be considerably affected by the drug, as observed by DLS measurements and SEM measurements. Table 1 reflects that the CUR/PEDOT NPs are small and monodisperse (*i.e.* $D_{eff}$ with low standard deviation), whereas PIP/PEDOT NPs are relatively large and polydisperse (*i.e.* $D_{eff}$ with high standard deviations). The yielded NPs and their corresponding aggregates successfully remained below 4 μm, which is the smallest diameter of human blood capillaries,[29] and thus avoiding the blockage of blood vessels or the possibility of being eliminated by the body reticuloendothelial system.

SEM and DLS observations are corroborated by the atomic force microscopy (AFM) images displayed in Figure 3, which reflect remarkable differences among PEDOT, CUR/PEDOT and PIP/PEDOT NPs. Thus, PEDOT NPs remained stable and very small while CUR/PEDOT and, especially, PIP/PEDOT exhibited higher size and tendency to aggregate. The size increment is probably due to the extremely low aqueous solubility of the two drugs, which promotes the formation of relatively large molecular cores inside PEDOT NPs. The tendency to aggregate is corroborated by the zeta- (ζ-) potential, which varies as follows: PEDOT < CUR/PEDOT < PIP/PEDOT (Table 1). The physical stability of an aqueous dispersion is considered to be good when the absolute value of the ζ-potential is around 30.[30] Therefore, the colloidal stability of

CUR/PEDOT and PIP/PEDOT NPs (ζ-potential of -26.5±5.1 and -18.7±3.0 mV, respectively) is lower than that of PEDOT NPs (-29.4±3.6 mV).

FTIR spectroscopy has been used to determine the chemical structure of the functional groups on the surface of PEDOT NPs. Figure 4 displays the FTIR spectra recorded for drugs, PEDOT NPs and drug/PEDOT NPs. PEDOT NPs doped with DBSA exhibit the main absorption peaks from the thiophene, ether and sulfonate groups: stretching modes of C=C in the thiophene ring at 1647 and 1557 $cm^{-1}$, $CH_2$ stretching modes at 1478, 1396 and 750 $cm^{-1}$, C–O–C vibrations at 1206 and 1057 $cm^{-1}$, and the S–O stretch at 667 $cm^{-1}$.

The addition of drugs during the polymerization process did not affect the localization of PEDOT bands; instead, the bands associated to the individual drugs were appreciated proving their incorporation. The two main characteristic C=O stretching bands at 1626 and 1535 $cm^{-1}$ and the enol C–O peak at 1267 $cm^{-1}$ observed for CUR alone are also detected in CUR/PEDOT NPs (Figure 4a). Similarly, the very broad band at 3293 $cm^{-1}$ and the sharp peak at 3508 $cm^{-1}$ indicate the presence of OH, whereas the peaks at 959 and 713 $cm^{-1}$ have been attributed to the benzoate *trans*- and *cis*-CH vibrations, respectively. Finally, the FTIR spectrum of free PIP (Figure 4b) clearly shows the characteristic C=O stretching peaks at 1628 and 1545 $cm^{-1}$, which are preserved in PIP/PEDOT NPs.

Dialysis bags with a molecular weight cut-off of 3500 KDa were used to understand the kinetics of the non-stimulated drug release in different media (Figure 5). In order to achieve a complete CUR and PIP release, three different environments with increasing affinity for the drug were examined: PBS with 0.5% Tween 20 (which is a surfactant that helps the dissolution of the drug), and the same solution mixed with 10% ethanol (EtOH) and with 70% EtOH. Comparison of the released amount of drug from

drug/PEDOT NPs with their respective controls (*i.e.* drugs alone) allows to visualize a different behaviour for CUR and PIP when interact with PEDOT. More specifically, the release of CUR from CUR/PEDOT NPs was much slower than that of PIP from PIP/PEDOT NPs with respect to their corresponding controls. These results reflect a relatively strong interaction between CUR and PEDOT, making difficult the release of the drug from the NPs until an environment with a high alcoholic content is used (Figure 5a). Instead, the release of PIP from the NPs was very similar to that of the control, indicating a simple diffusion phenomenon motivated by the poor affinity between the drug and the ECP. This feature is confirmed by the almost imperceptible effect of the increment of EtOH in the release medium (Figure 5b). The divergent behaviour of CUR/PEDOT and PIP/PEDOT should be attributed to the different hydrogen bonding abilities of the two drugs. Thus, CUR⋯PEDOT hydrogen bonds are expected to be formed between the hydroxyl groups of CUR (Figure 1c) and the dioxane rings of PEDOT. It should be noted that this kind of specific interactions were found to play a crucial role in DNA⋯PEDOT interactions,[31] which are highly dependent on the DNA sequence. In contrast, the absence of groups able to act as hydrogen bonding donors in PIP precludes the formation of PIP⋯PEDOT hydrogen bonding interactions. Overall, these results suggest that CUR/PEDOT NPs are promising candidates to behave as electrically responsive drug delivery systems.

Before of the electrostimulation studies, the electrochemical response of CUR, PIP, and both PEDOT and drug/PEDOT NPs was examined by cyclic voltammetry (CV), registering oxidation–reduction cycles within the potential range of -1.5 to + 1 V at different scan rates. Figure 6a (left) displays a photograph of the three electrode configuration when cyclic voltammetry was recorded from CUR/PEDOT NPs deposited

on GCE. Interestingly, it was possible to visualize the release of CUR from the NPs when low scan rates were employed.

Cyclic voltammograms recorded for CUR and PIP are displayed in Figures S3a and S3b, respectively. Since CUR molecule contains two hydroxyl groups a conjugation effect can occur from the electron cloud deviation. As can be it seen CUR exhibits one well defined anodic peak at a potential of ~ +0. 4 V and a less defined cathodic peak at ~ -0.10 V (Figure S3a), which are similar to that previously observed elsewhere.[32]. These quasi-reversible peaks have been attributed to the product of the irreversible oxidation reaction, which can be adsorbed onto the electrode surface. The intensity of the peaks increases in absolute value with the scan rate and, in addition, the peaks potential shift slightly indicating that they correspond to a quasi-reversible redox process.[33] Instead, the voltammograms recorded for PIP exhibit two irreversible anodic peaks at 0.12 V and 0.92 V.

Cyclic voltammograms of PEDOT, CUR/PEDOT and PIP/PEDOT NPs adsorbed onto glassy carbon electrodes are compared in Figures 6b-d. The current density increases proportionally with the scan rate suggesting that the electrochemical process depends on the difussion.[34] Moreover, detailed inspection of the voltammograms recorded for CUR/PEDOT NPs allows identification of the CUR anodic peak at a potential between 0.4 and 0.5 V, depending on the scan rate. Figure 6e plots the current density at the anodic and cathodic peaks ($j_p$) of CUR against the square root of the scan rate, while Figure 6f represents the same graphic for the irreversible anodic process of PIP at 0.92 V. A linear behavior is observed in all cases. Moreover, in the case of CUR the slope was slightly higher for the anodic process than for the cathodic one. These results confirm the dependence of electrode reaction on the diffusion, which is the mass

transport rate of the electroactive species to the surface of the electrode across a concentration gradient.

Experiments with electrostimulation were performed using a conventional three-electrode setup, similar to that displayed in Figure 6a, with glassy carbon coated with drug/PEDOT NPs as working electrode (WE), bare glassy carbon as counter electrode (CE), and Ag|AgCl as reference electrode (RE). To investigate the effect of the voltage on the release of CUR and PIP from drug/PEDOT NPs, different voltages (*i.e.* 0.50 V, −0.50 V, −1.00 V and −1.25 V) were applied during 3 min. Results have been compared with control experiments, which were performed in absence of electric voltage (hereafter denoted 0.00 V). In order to mimic a physiological medium, electrically stimulated drug release experiments were performed using PBS 1 with 0.5 % (v/v) Tween 20 at pH 7.4 as electrolyte medium.

Results found for CUR and PIP, which are displayed in Figures 7a and 7b, respectively, demonstrate completely different behaviours. The percentage of released CUR with respect to the amount of encapsulated CUR was lower than 5% when the applied voltage was 0.50 V or in absence of stimulus, while increased progressively and linearly with the more negative voltage. Thus, the stimulation with −1.25 V for 3 min resulted in a CUR delivery of 38%. In the case of PIP/PEDOT NPs, the amount of released drug in absence of stimulus is 10%, increasing to 18% and 23% when the applied voltage is −0.50 and 0.50 V, respectively. No systematic behaviour was identified in the case of PIP (Figure 7b), indicating that the release of this drug cannot be controlled and programmed through electrostimulation.

Figures 7c and 7d display the release of CUR and PIP, respectively, from drug/PEDOT NPs with time. Results from these experiments, which were performed using a fixed voltage of −1.25 V, are consistent with those reported in Figures 7a and

7b, indicating that controlled release by electrical stimulation can be efficiently achieved only for CUR. Thus, although 7% of CUR is released after 30 s only, the amount of released drug increases logarithmically with time. In the time interval compressed between 3 and 9 min, the release grows from 38% to 60%. Also, complementary assays showed that the CUR release stops when the voltage is tuned off, proving that this is a regulated process. These results reflect that the controlled CUR release can be achieved with both time and applied potential (Figures 7a and 7c, respectively). Release profiles were reproducible not only with as fresh samples but also with suspensions that were stored for even one month before the release assays. The variation of PIP release with time is practically null (*i.e.* 20% after both 3 and 9 min), corroborating that the poor interactions between such drug and the ECP preclude the applicability of PIP/PEDOT NPs as dosage-controlled drug delivery vehicles.

Previous studies suggested that the take-up and rate delivery of drugs may depend on the structure, composition and oxidation state of the ECP.[11] In the particular case of the release of charged drugs by electrical stimulation, the main factor is the oxidation state since the driving force of this process is the apparition of repulsive drug⋯ECP electrostatic interactions. Thus, the oxidation and reduction of the ECP cause the release of cationic and anionic drugs, respectively.[11] However, CUR and PIP are neutral drugs at pH= 7 and, therefore, their electrically stimulated release is expected to be controlled by a more complex mechanism. Unfortunately, designs allowing for the controlled release of neutral drugs are very scarce. Langer and co-workers[35] used biotin-doped PPy to load biotinylated nerve growth factor (NGF) at the biotin binding sites found at the polymer surface. Reduction of the PPy film resulted in an electrically triggered NGF release, which remained biologically active. On the other hand, N-methylphenpthiazine

(NMP) loaded into PPy doped with anionic β-cyclodextrins was released when oxidized, which caused the formation of positive charges on both the ECP and NMP.[36]

The mechanism proposed in this work for the electrically stimulated release of CUR is based on the effect of the voltage on the oxidation state of the ECP and, therefore, on PEDOT⋯CUR interactions. The release of CUR is not stimulated by the application of the positive voltage (+0.50 V), which enhances the positive oxidation state of the polymer (Figure S3) while the oxidation of the drug starts at around such potential (Figure S3). In contrast, the CUR release becomes electrostimulated upon the application of negative voltages, which induce the electrochemical de-doping (reduction) of PEDOT NPs. Thus, the fraction of reduced PEDOT sites over the number of total active sites (*i.e.* where electrons are exchanged) increases with the negative voltage, polymer chains being expected to be completely, or almost completely, reduced (*i.e.* de-doped – with neutral charge) at the voltage of –1.25 V.[34] It was observed that lower voltages caused mechanical and electrochemical degradation of the ECP NPs. The de-doping of the ECP affects the intermolecular interactions with the drug, hydrogen bonds being significantly weaker when PEDOT chains are in the neutral state than in the oxidized state.[37] Accordingly, the mechanism for the electrostimulated CUR release from CUR/PEDOT NPs can be summarized by the following Eqn:

$$(\mathrm{PEDOT}^{\alpha+}\cdot \alpha\mathrm{DBSA}^{-})\cdots n\mathrm{CUR} + \beta\mathrm{e}^{-} \rightarrow$$

$$(\mathrm{PEDOT}^{(\alpha-\beta)+}\cdot(\alpha-\beta)\mathrm{DBSA}^{-})\cdots m\mathrm{CUR} + \beta\mathrm{DBSA}^{-} + (n-m)\mathrm{CUR}$$

where *n*CUR refers to the drug molecules hydrogen bonded to the oxidized polymeric NPs, *m*CUR corresponds to the drug molecules that remain hydrogen bonded to the polymeric NPs after pump $\beta$ electrons into the system by electrical stimulation, and $\alpha$+ and ($\alpha$-$\beta$)+ are the oxidation states of oxidized and reduced PEDOT,

respectively (*i.e.* when PEDOT is completely reduced, $\alpha=\beta$, the charge of the ECP is zero.

The release mechanism proposed in this work for neutral drugs able to form specific interactions with the ECP matrix resembles that typically reported when negatively charged drugs act as dopant ions.[8] Unfortunately, this mechanism does not apply to PIP/PEDOT NPs because of the lack of hydrogen bonding donors in the drug. Accordingly, PIP molecules are rapidly released by through the walls of the polymeric NPs, such diffusion process being independent of the presence or not of external stimuli. Thus, although the application of an electric voltage affects the oxidation state of PEDOT chains, it does not improve the control in the release that is determined by the intrinsically weak dispersion interactions between PIP molecules and the aromatic rings of the ECP.

In order to overcome the limitations associated to the instability in the light, poor oral bio-availability in vivo and lack of solubility in aqueous solvents of CUR, the use of micro- and nanoparticles made of polymer materials, as for example poly(lactic-*co*-glycolic acid), as carriers has been extensively explored.[38] Although polymeric micro- and nanoparticles provided biocompatibility, in some cases also biodegradable, platforms for sustained release of CUR with improved bio-availability, several disadvantages were detected. The most important one, which is the effective control during the release, has been overcome in this work applying a controlled voltage to electrodes coated with CUR/PEDOT NPs, achieving a programmed CUR release.

The biocompatibility and cytotoxicity of such system is an important characteristic to be analyzed for further biological applications. PEDOT NPs and the surfactant (DBSA) alone were tested in epithelial-like prostate and breast adenocarcinoma cells lines from human (PC3 and MCF-7, respectively) using the MTT assay measured after 24 h post-

treatment (Figure 8a). PEDOT NPs do not exhibit any toxic effect until they are used at high concentration. Moreover, it is clearly demonstrated that, after the 3 washing steps, the quantity of dopant is lower than 6 µg/mL, when DBSA starts to be toxic. The cytotoxicity of free CUR and CUR/PEDOT NPs, which was evaluated at 24 h post-treatment using the same cell lines, reflects significant concentration dependence (Figure 8b). Significant differences are observed in the behaviour of the two systems, free CUR being considerably more toxic than CUR/PEDOT NPs. More specifically, for PC3 the half-maximal inhibitory concentration (IC50) of the former and the latter is around 20 and 100 µg/mL, respectively, while for MCF-7 both are around 10 µg/mL. These results, combined with the fact that the drug loaded inside the NPs is only partially released in absence of external stimuli, corroborate that PEDOT nanostructures formed by emulsion polymerization is a very interesting electroactive vehicle for the controlled delivery of neutral drugs having groups able to interact with hydrogen bonds.

In order to explore the mechanisms of cytotoxicity, the cellular uptake of free CUR and CUR/PEDOT NPs on PC3 and MCF-7 cells was observed by fluorescence microscopy. Figure 9 shows the images of non-treated cells, PEDOT NPs treated, free CUR treated and CUR/PEDOT treated for 24 h. Medium without treatment drug was regarded as control, as well as, the PEDOT NPs treated group. Both groups did not present any fluorescence at any point and there was not any diminish in cell nucleus number. In contrast, an intense fluorescence was observed at the cell cytosol after 24 h for free CUR and CUR/PEDOT NPs. In addition, the two groups exhibited lower number of cell nuclei than before the treatment had been executed. Besides, different cellular morphologies were observed: cells treated with free CUR presented more rounded bodies, denoted by high circularity (Figure 9c), than cells treated with CUR/PEDOT. These results suggest that cells were more affected by free CUR than

when it is encapsulated within the PEDOT NPs, again indicating that the complete effect of the drug would not be achieved until it is stimulated.

Overall, results obtained in this paper indicate that CUR/PEDOT NPs can be considered as potential controlled release systems for therapeutic applications based on the anti-bacterial, anti-viral, anti-protozoal, anti-inflammatory or anti-cancer activity of CUR. This system allows a given dosage at desired periodical time by applying a harmless external voltage of only -1.25 V (*i.e.* from a conventional small battery). Moreover, after its optimization to reduce a little bit more the required voltage, one could envision advanced biomedical applications of the CUR/PEDOT NPs system using the weak electric fields naturally occurring in the body for stimulation (*e.g.* the intrinsic electric fields of cardiovascular and neuronal tissues).

## 3. Conclusions

Encapsulation of CUR and PIP in PEDOT NPs was achieved by *in situ* emulsion polymerization using DBSA as stabilizer and doping agent. The release behaviour of these two neutral drugs, which only differ in their capacity to form hydrogen bonding interactions with the oxidized polymer chains, was very different in absence and in presence of external electrostimulation. The release of CUR is controlled through the strength of such specific drug···ECP interactions, which become weaker when polymer chains are reduced applying an external negative voltage. Therefore, CUR/PEDOT NPs are a promising combination that efficiently controls the release of the drug through external stimuli. This methodology, which can be extrapolated to other neutral drugs with similar hydrogen bonding abilities, may be a potential strategy for treatments based on the programmed dosage of CUR that, among many other medicinal properties, have

demonstrated efficacy as anticancer agent for many types of malignancies, including colorectal, breast, lung, prostate, and pancreatic carcinoma.[22d]

## Acknowledgements

Authors acknowledge MINECO/FEDER (MAT2015-69367-R) for financial support. C.A. is grateful to ICREA Academia program.

## References

[1] a) G. Baolin, L. Glavas, A.-C. Albertsson, *Prog. Polym. Sci.* **2013**, *38*, 1263; b) T. Darmanin, F. Guittard, *Prog. Polym. Sci*. **2014**, *39*, 656; c) J. Heinze, B. A. Frontana-Uribe, S. Ludwigs, *Chem. Rev.* **2010**, *110*, 4724; d) A. Guiseppi-Elie, *Biomaterials* **2010**, *31*, 2701; e) T. F. Otero, J. G. Martínez, J. Arias-Pardilla, *J. Electrochim. Acta* **2012**, *84*, 112.

[2] a) M. M. Pérez-Madrigal, E. Armelin, J. Puiggalí, C. Alemán, *J. Mater. Chem. B* **2015**, *3*, 5904; b) R. Green, M. R. Abidian, *Adv. Mater.* **2015**, *27*, 7620; c) Z. H. Wang, P. Tammela, J. X. Huo, P. Zhang, M. Stromme, L. Nyholm, *J. Mater. Chem. A* **2016**, *4*, 1714; d) D. E: López-Pérez, D. Aradilla, L. J. del Valle, C. Alemán, *J. Phys. Chem. C* **2013**, *117*, 6607.

[3] a) W. K. Wan, L. Yang, D. T. Padavan, *Nanomedicine* **2007**, *2*, 483; b) B. P. Timko, D. S. Kohane, *Clin. Ther.* **2012**, *34*, S25.

[4] D. A. LaVan, T. McGuire, R. Langer, *Nat. Biotechnol.* **2003**, *21*, 1184.

[5] a) S. Mura, J. Nicolas, P. Couvreur, *Nat. Mater.* **2013**, *12*, 991; b) B. P. Timko, T. Dvir, D. S. Kohane, *Adv. Mater.* **2010**, *22*, 4925; c) S. C. Balmert, S. R. Little, *Adv. Mater*. **2012**, *24***,** 3757.

[6] J. Neofytou, E. Ge, T. J. Cahill, R. E. Beygui, R. N. Zare, *ACS Nano* **2012**, *6*, 227.

[7] a) N. Hosseini-Nassab, D. Samnta, Y. Abdolazimi, J. P. Annes, R. N. Zare, *Nanoscale* **2017**, *9*, 143; b) Y. L. Yang, X. J. Zhang, C. T. Yu, X. J. Hao, J. S. Jie, M. J. Zhou, X. H. Zhang, *Adv. Healthcare Mater.* **2014**, *3*, 906.

[8] D. Svirskis, J. Travas-Sejdic, A. Rodgers, S. Garg, *J. Controlled Release*. **2010**, *146*, 6.

[9] a) R. Wadhwa, C. F. Lagenaur, X. T. Cui, *J. Control Release*. **2006**, *110*, 531; b) L. L. Miller, X. U. Zhou, *Macromolecules* **1987**, *20*, 1594; c) G. Stevenson, S. E. Moulton, P. C. Innis, G. G. Wallace, *Synth. Met.* **2010**, *160*, 1107

[10] G. Jeon, S. Y. Yang, J. Byun, J. K. Kim, *Nano Lett.* **2011**, *11*, 1284.

[11] B. Alshammary, F. C. Walsh, P. Herrasti, J. C. Ponce de Leon, *J. Solid State Electrochem*. **2016**, *20*, 3375.

[12] G. M. Whitesides, *Nat. Biotechnol*. **2003**, *21*, 1161.

[13] D. D. Ateh, H. A. Navsaria, P. Vadgama, *J. R. Soc. Interface* **2006**, *3*, 741.

[14] D. Samanta, N. Hosseini-Nassab, R. N. Zare, *Nanoscale* **2016**, **8**, 9310.

[15] a) D. Samanta, J. L. Meiser, R. N. Zare, *Nanoscale* **2015**, *7*, 9497; b) Y. Wang, Y. Xiao, R. Tang, *Chem. Eur. J.* **2014**, *20*, 11826; c) D. Park, Y. Cho, S.-H. Goh, Y. Choi, *Chem. Commun*. **2014**, *50*, 15014.

[16] a) L. Groenendaal, G. Zotti, P.-H. Aubert, S. M. Waybright, J. R. Reynolds, *Adv. Mater*. **2003**, *15*, 855; b) L. Groenendaal, F. Jonas, D. Freitag, H. Pielartzik, J. R. Reynolds, *Adv. Mater*. **2000**, *12*, 481; c) S. Kirchmeyer, K. Reuter, *J. Mater. Chem*. **2005**, *15*, 2077; d) L. J. del Valle, F. Estrany, E. Armelin, R. Oliver, C. Alemán, *Macromol. Biosci.* **2008**, *8*, 1144.

[17] D. Aradilla, F. Estrany, C. Alemán, *J. Phys. Chem. C* **2011**, *115*, 8430.

[18] a) Y. Shi, L. Peng, G. Yu, *Nanoscale* **2015**, *7*, 12796; b) R. A. Green, N. H. Lovell, G. G. Wallace, L. A. Poole-Warren, *Biomaterials* **2008**, *29*, 3393; c) M. R. Abidian, J.

M. Corey, D. R. Kipke, D. C. Martin, *Small* **2010**, *6*, 421; d) B. Winther-Jensen, O. Winther-Jensen, M. Forsyth, D. R. MacFarlane, *Science* **2008**, *321*, 671; e) G. Fabregat, B. Teixeira-Dias, L. J. del Valle, E. Armelin, F. Estrany, C. Alemán, *ACS Appl. Mater. Interfaces* **2014**, *6*, 11940.

[19] a) C. Alemán, J. Casanovas, J. Torras, O. Bertran, E. Armelin, R. Oliver, F. Estrany, *Polymer* **2008**, *49*, 1972; D. Aradilla, F. Estrany, E. Armelin, C. Alemán, *Thin Solid Films* **2010**, *518*, 4203.

[20] N. Paradee, A. Sirivat, *J. Phys. Chem. B* **2014**, *118*, 9263.

[21] D. Liu, L. Ma, Y. An, Y. Li, Y. Liu, L. Wang, J. Guo, J. Wang, J. Zhou, *Adv. Funct. Mater*. **2016**, *26*, 4749.

[22] a) D. Karunagaran, R. Rashmi, T. R. Kumar, *Curr. Cancer Drug Targets*. **2005**, 5, 117; b) C. H. Hsu, A. L. Cheng, *Adv. Exp. Med. Biol.* **2007**, *595*, 471; c) B. B. Aggarwal, B. Sung, *Trends Pharmacol. Sci.* **2009**, 30, 85; d) P. Anand, A. B. Kunnumakkara, C. Sundaram, K. B. Harikumar, B. Sung, S. T. Tharakan, K. Misra, I. K. Priyadarsini, K. N. Rajasekharan, B. B. Aggarwal, *Biochem. Pharmacol.* **2008**, *76*, 1590.

[23] a) M. B. Daware, A. M. Mujumdar, S. Ghaskadbi, *Planta Med* **2000**, *66*, 231; b) S. H. Kim, Y. C. Lee, *J. Pharm. Pharmacol.* **2009**, *61*, 353; c) R. S. Vijayakumar and N. Nalini, *Cell Biochem. Funct*. **2006**, *24*, 491.

[24] M. Marti, G. Fabregat, F. Estrany, C. Aleman, E. Armelin, *J. Mater. Chem.* **2010**, *20*, 10652; b) M. G. Han and S. H. Foulger, *Chem. Commun.* **2004**, *19*, 2154; c) S. C. Luo, H. H. Yu, A. C. Wan, Y. Han, J. Y. Ying, *Small* **2008**, *4*, 2051.

[25] T. L. Kelly, M. O. Wolf, *Chem. Soc. Rev.* **2010**, *39*, 1526.

[26] L. Li, Y. Liu, P. Hao, Z. Wang, Li. Fu, Z. Ma, J. Zhou, *Biomaterials* **2015**, *41*, 132.

[27] L. Fielding, J. K. Hillier, M. J. Burchell, S. P. Armes, *Chem. Commun.* **2015**, *51*, 16886.

[28] X. Yang, Z. Li, N. Wang L. Li, L. Song, T. He, L. Sun, Z. Wang, Q. Wu, N. Luo, C. Yi, C. Gong, *Sci. Rep.* **2015**, *5*, 10322.

[29] T. Neuberger, B. Schöpf, H. Hofmann, M. Hofmann, B. Von Rechenberg, *J. Magn. Magn. Mater.* **2005**, *293*, 483.

[30] a) S. A. Wissing, O. Kayser, R. H. Müller, *Adv. Drug Deliver. Rev*. **2004**, *56*, 1257; b) C. Jacobs, O. Kayser, R. H. Müller, *Int. J. Pharm*. **2000**, *196*, 161.

[31] a) B. Teixeira-Dias, D. Zanuy, J. Poater, M. Solà, F. Estrany, L. J. del Valle, C. Alemán, *Soft Matter* **2011**, *7*, 9922; b) D. Zanuy, B. Teixeira-Dias, L. J. del Valle, J. Poater, M. Solà, C. Alemán, *RSC Adv.* **2013**, *3*, 2639.

[32] a) D. Zhang, X. Ouyang, J. Ma, L. Li, Y. Zhang, *Electroanalysis* **2016**, *28*, 749; b) N. S. Jha, S. Mishra, S. K. Jha, A. Surolia, *Electrochim. Acta.* **2015**, *151*, 574.

[33] K. Li, Y. Li, L. Yang, L. Wang, B. Ye, *Anal. Methods* **2014**, *6*, 7801.

[34] M. Marzocchi, I. Gualandi, M. Calienni, I. Zironi, E. Scavetta, G. Castellani, B. Fabroni, *ACS Appl. Mater. Interfaces* **2015**, *7*, 17993.

[35] P. M. George, D. A. LaVan, J. A. Burdick, C.-Y. Chen, E. Liang, R. Langer, *Adv. Mater*. **2006**, *18*, 577–581.

[36] G. Bidan, C. Lopez, F. Mendes-Viegas, E. Vieil, *Biosens. Bioelectron*. **1994**, *9*, 219.

[37] B. Teixeira-Dias, D. Zanuy, L. J. del Valle, F. Estrany, E. Armelin, C. Alemán, *Macromol. Chem. Phys.* **2010**, *211*, 1117.

[38] a) M. A. N. Manaia, V. C. Diculescu, E. S. Gil, A. M. Oliveira-Brett, *J. Electroanal. Chem*. **2012**, *682*, 83; b) J. M. Chan, L. Zhang, K. P. Yuet, G. Liao, J.-W.

Rhee, R. Langer, *Biomaterials* **2009**, *30*, 1627; c) S. Yuan, F. Lei, Z. Liu, T. Si, R. X. Xu, *PLOS One* **2015**, *10*, e0132609

**Table 1.** Effective diamerter ($D_{eff}$) determined by SEM and DLS, drug loading ratio (DLR) and ζ-potential of unloaded-PEDOT, CUR/PEDOT and PIP/PEDOT NPs.

| | **$D_{eff}$ *(nm)* SEM** | **$D_{eff}$ *(nm)* DLS** | **DLR (%)** | **ζ-potential (mV)** |
|---|---|---|---|---|
| PEDOT | 35±6 | 84±2 | - | -29.4±3.6 |
| CUR/PEDOT | 96±16 | 207±3 | 5.9±1.6 | -26.5±25.1 |
| PIP/PEDOT | 292±132 | 304±17 | 8.0±0.4 | -18.7±3.0 |

## CAPTIONS TO FIGURES

**Figure 1.** (a) Schematic representation of the chemical synthesis of PEDOT NPs by emulsion polymerization. (b) Trasmision electron microscopy (TEM) micrographs of PEDOT NPs obtained using the procedure displayed in (a). (c) Chemical structure of CUR and PIP.

**Figure 2.** SEM images of (a) CUR/PEDOT NPs and (b) PIP/PEDOT NPs (Scale bar: 200 nm). Effective diameter histograms derived from SEM measurements and average values are also displayed.

**Figure 3.** AFM images (1×1 $\mu m^2$) of (a) PEDOT, (b) CUR/PEDOT and (c) PIP/PEDOT NPs. The graphs displayed in panels (d-e) corresponds to the profile of the selected particles.

**Figure 4.** FTIR spectra of (a) PEDOT NPs, CUR and CUR/PEDOT NPs; and (b) PEDOT NPs, PIP and PIP/PEDOT NPs.

**Figure 5.** Cumulative drug release comparison between drug/PEDOT NPs and free drug (control) dispersed in aquous solutions and dyalised against PBS+0.5% Tween 20, the previous PBS solution with 10% EtOH, and with 70% EtOH: (a) CUR and (b) PIP.

**Figure 6.** (a) Camera image of the three electrodes set-up for the electrochemical characterization of unloaded PEDOT and drug/PEDOT NPs. The red arrow points out released CUR in experiments with CUR/PEDOT NPs. WE, CE and RE refer to the working electrode, the counter electrode and the reference electrode, respectively. Cyclic voltammograms for (b) unloaded PEDOT NPs, (c) CUR/PEDOT NPs and (d) and PIP/PEDOT NPs recorded from –1.5 to 1.0 V at different varying scan rates (10, 20, 40, 60, 80, 100, 200, 300 and 400 mV/s) using PBS 1× (pH 7.4) as electrolyte medium. Variation of the current density ($j_p$) at the anodic and cathodic peaks (e) of CUR and at the anodic peak (f) of PIP against the square root of the scan rate.

**Figure 7.** Effect of (a,c) voltage with time constant (3 min) and (b,d) of time with voltage constant (-1.25 V) on drug release for drug/PEDOT NPs: (a,c) CUR and (b,d) PIP ($n$ = 6). The percentage of released drug is expressed with respect to the total amount of loaded drug.

**Figure 8.** (a) Cytotoxicity studies of PEDOT NPs and DBSA on PC3 amd MCF-7 cells for 24 h. Although they are represented in the same graphic, assays with PEDOT NPs and DBSA were performed independently. (b) Cytotoxicity evaluation of CUR and CUR/PEDOT NPs on PC3 and MCF-7 cells for 24 h. Values are the mean of 3 samples and bars indicate their standard deviation. Greek letters on the columns/points refer to significant differences when the 2-way ANOVA and Tukey's multiple comparisons test are applied: α, δ, β indicate significant differences observed within the specific concentration group with $p$-values lower than 0.05, 0.001 and 0.0001, respectively.

**Figure 9.** (a) High magnification fluorescent images of PC3 and MCF-7 cells incubated with nothing (control), PEDOT NPs, CUR and CUR/PEDOT NPs for 24 h. Scale bars represent 40 μm. (b) Low magnification cell images of PC3 and MCF-7 incubated with CUR/PEDOT NPs for 24 h. Scale bars represent 100 μm. For each panel, the images from left to right showed cell nuclei stained by Hoechst (blue), CUR fluorescence (green) and overlays of both images. (d) Cell circularity assessed by ImageJ software. β indicates significant differences with a p-value lower than 0.0001 when a t-test is performed.

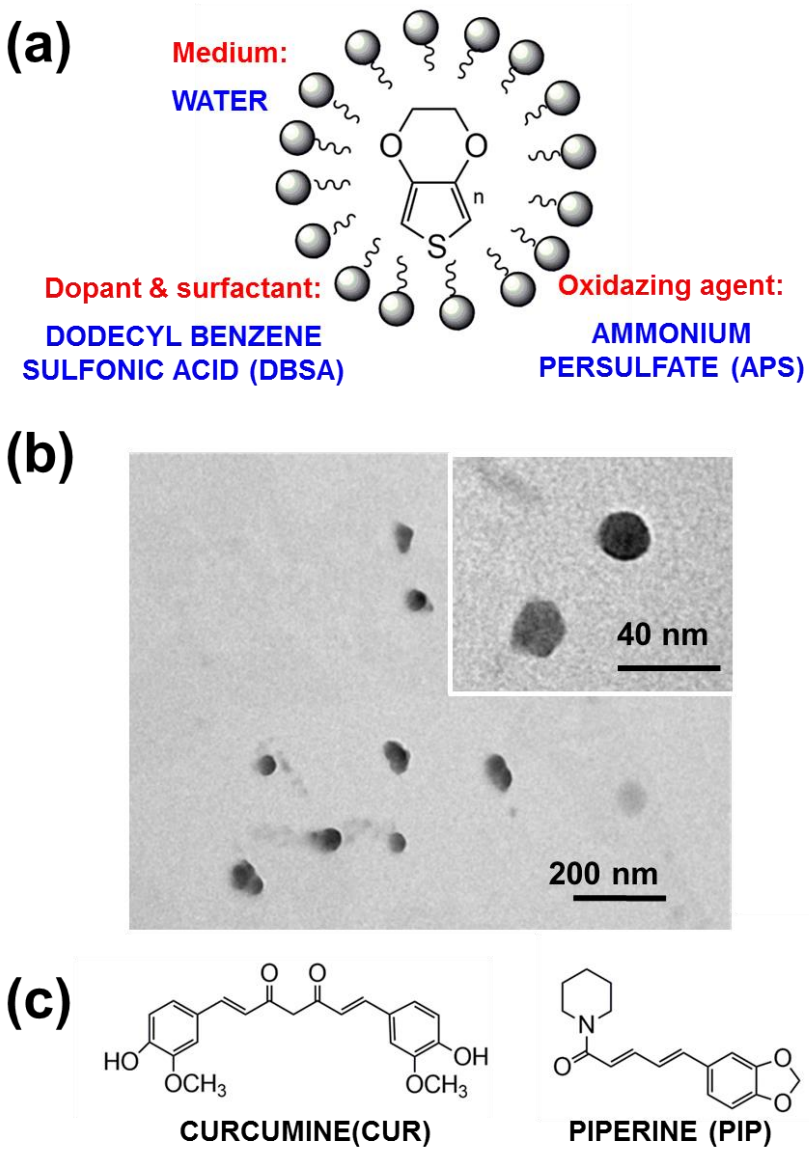
(a)
Medium:
WATER
Dopant & surfactant:
DODECYL BENZENE
SULFONIC ACID (DBSA)
Oxidazing agent:
AMMONIUM
PERSULFATE (APS)
(b)
40 nm
200 nm
(c)
CURCUMINE(CUR)
PIPERINE (PIP)

Figure 1

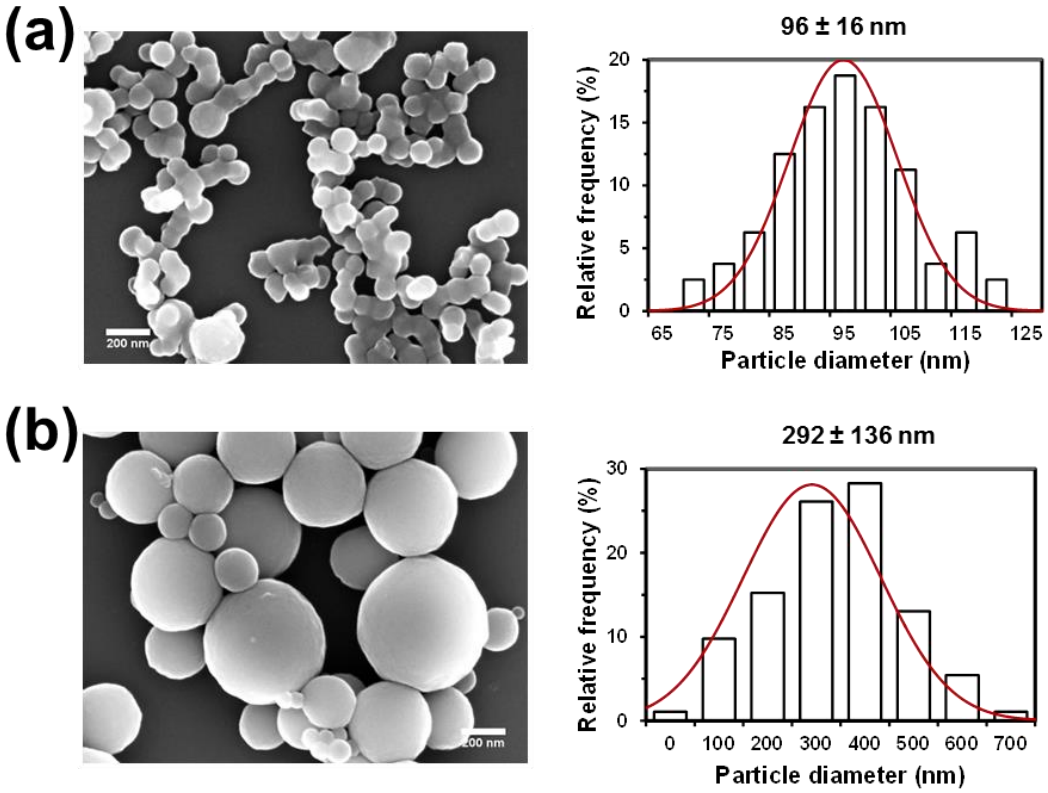
(a)
200 nm
96 ± 16 nm
Relative frequency (%)
0
5
10
15
20
65
75
85
95
105
115
125
Particle diameter (nm)
(b)
200 nm
292 ± 136 nm
Relative frequency (%)
0
10
20
30
0
100
200
300
400
500
600
700
Particle diameter (nm)

Figure 2

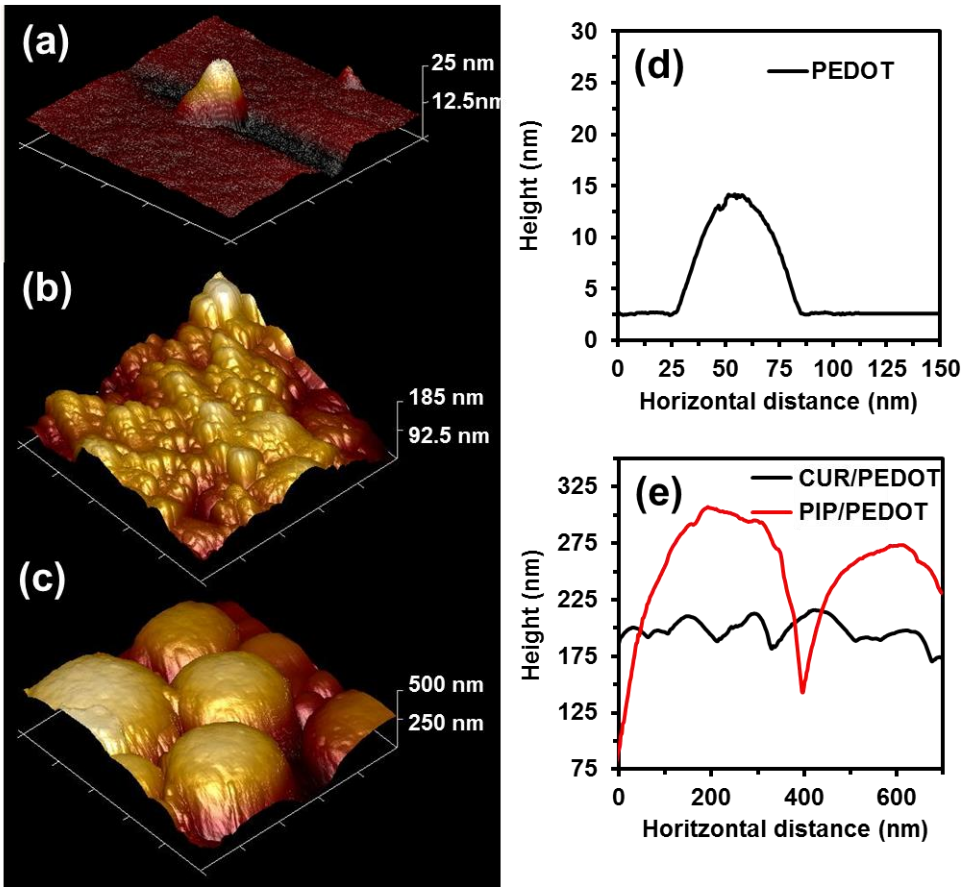
(a)
25 nm
12.5nm
(b)
185 nm
92.5 nm
(c)
500 nm
250 nm
(d)
PEDOT
Height (nm)
Horizontal distance (nm)
(e)
CUR/PEDOT
PIP/PEDOT
Height (nm)
Horitzontal distance (nm)

Figure 3

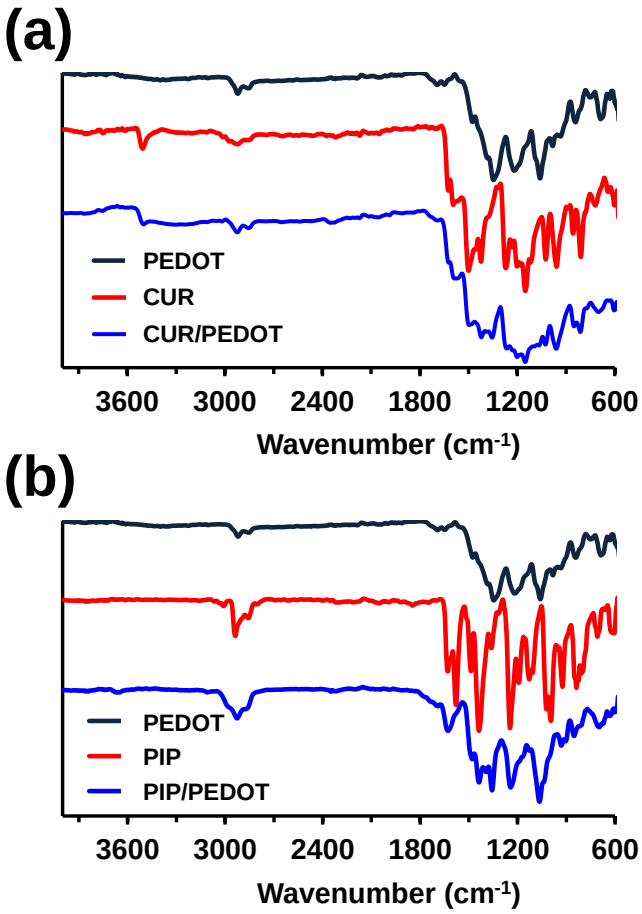
(a)
PEDOT
CUR
CUR/PEDOT
3600
3000
2400
1800
1200
600
Wavenumber (cm-1)
(b)
PEDOT
PIP
PIP/PEDOT
3600
3000
2400
1800
1200
600
Wavenumber (cm-1)

Figure 4

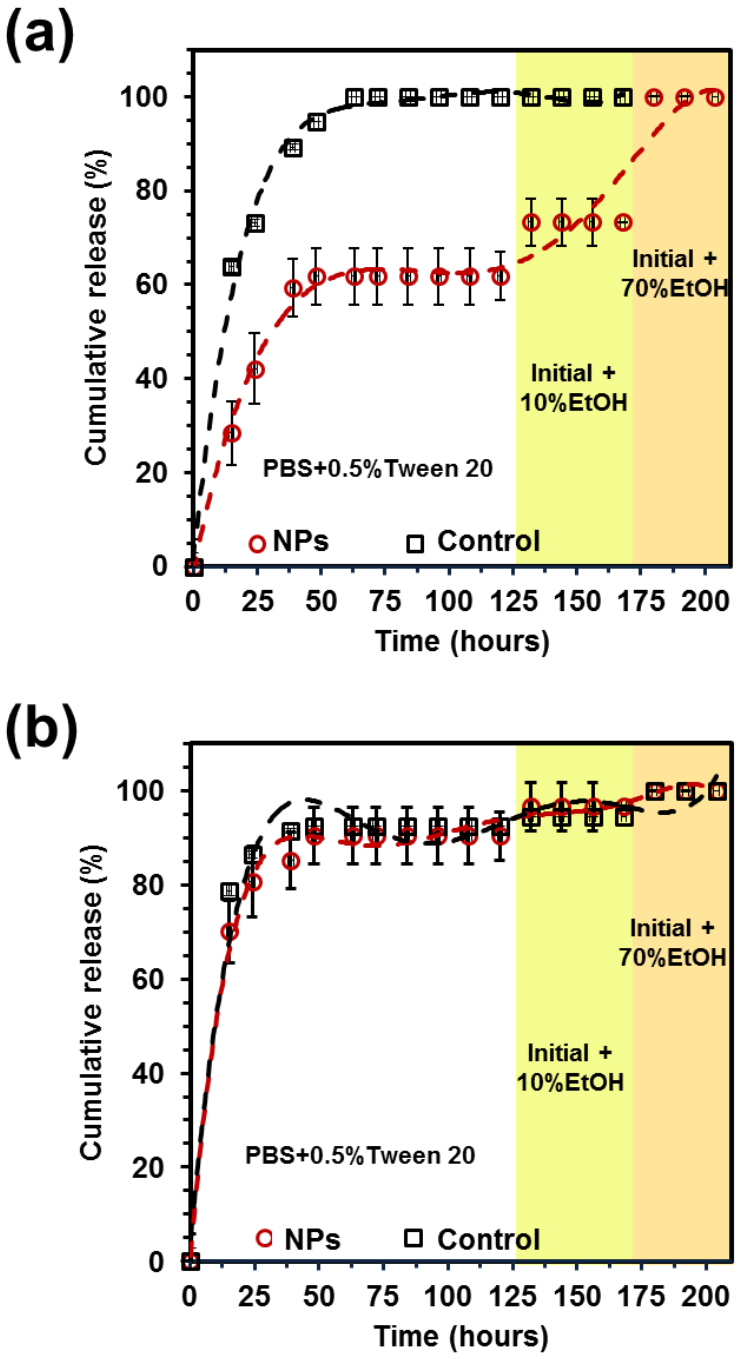
(a)
Cumulative release (%)
100
80
60
40
20
0
0 25 50 75 100 125 150 175 200
Time (hours)
Initial +
70%EtOH
Initial +
10%EtOH
PBS+0.5%Tween 20
NPs
Control
(b)
Cumulative release (%)
100
80
60
40
20
0
0 25 50 75 100 125 150 175 200
Time (hours)
Initial +
70%EtOH
Initial +
10%EtOH
PBS+0.5%Tween 20
NPs
Control

Figure 5

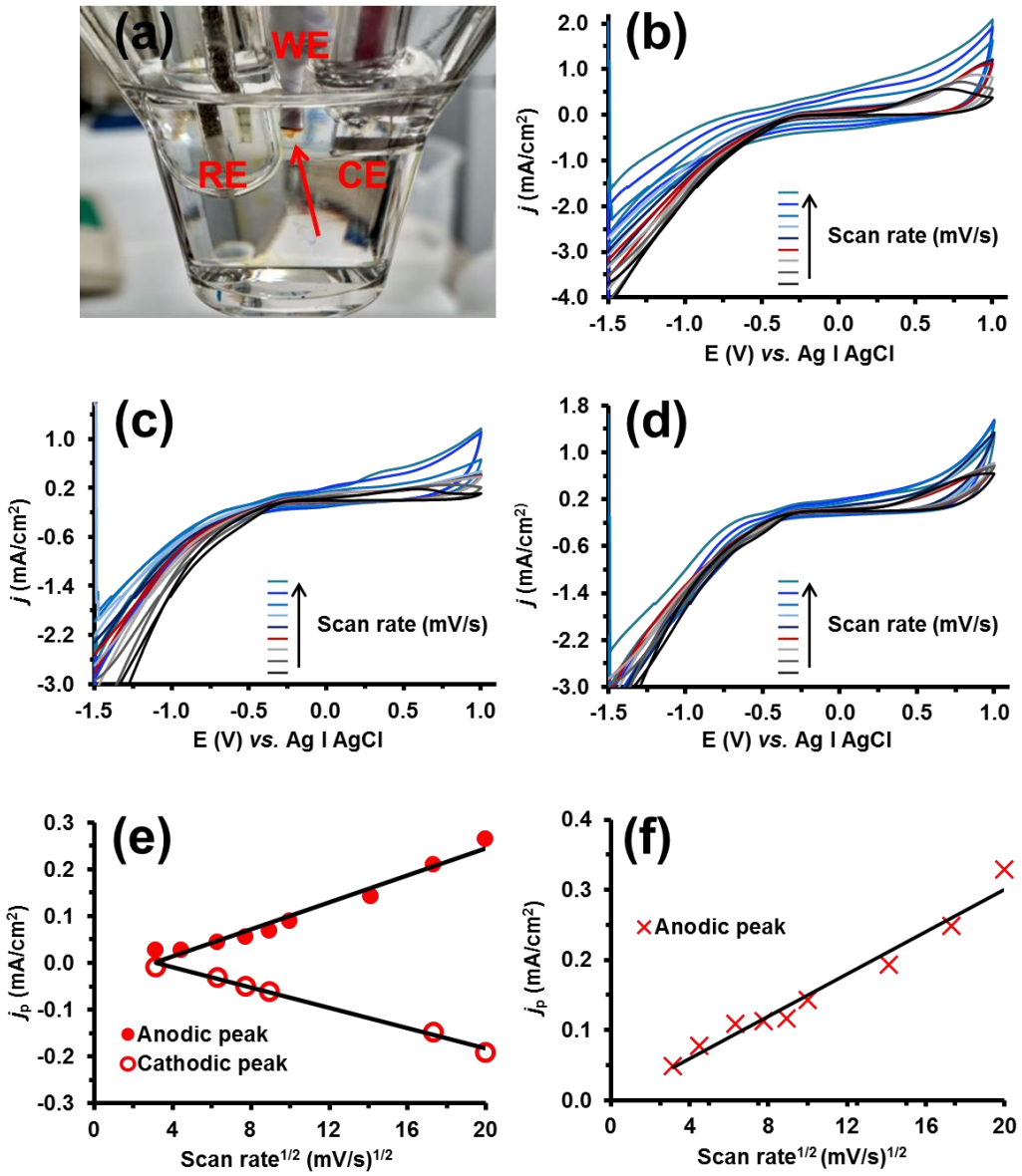
(a)
WE
RE
CE
(b)
j (mA/cm²)
Scan rate (mV/s)
E (V) vs. Ag I AgCl
(c)
j (mA/cm²)
Scan rate (mV/s)
E (V) vs. Ag I AgCl
(d)
j (mA/cm²)
Scan rate (mV/s)
E (V) vs. Ag I AgCl
(e)
jp (mA/cm²)
Anodic peak
Cathodic peak
Scan rate1/2 (mV/s)1/2
(f)
jp (mA/cm²)
Anodic peak
Scan rate1/2 (mV/s)1/2

Figure 6

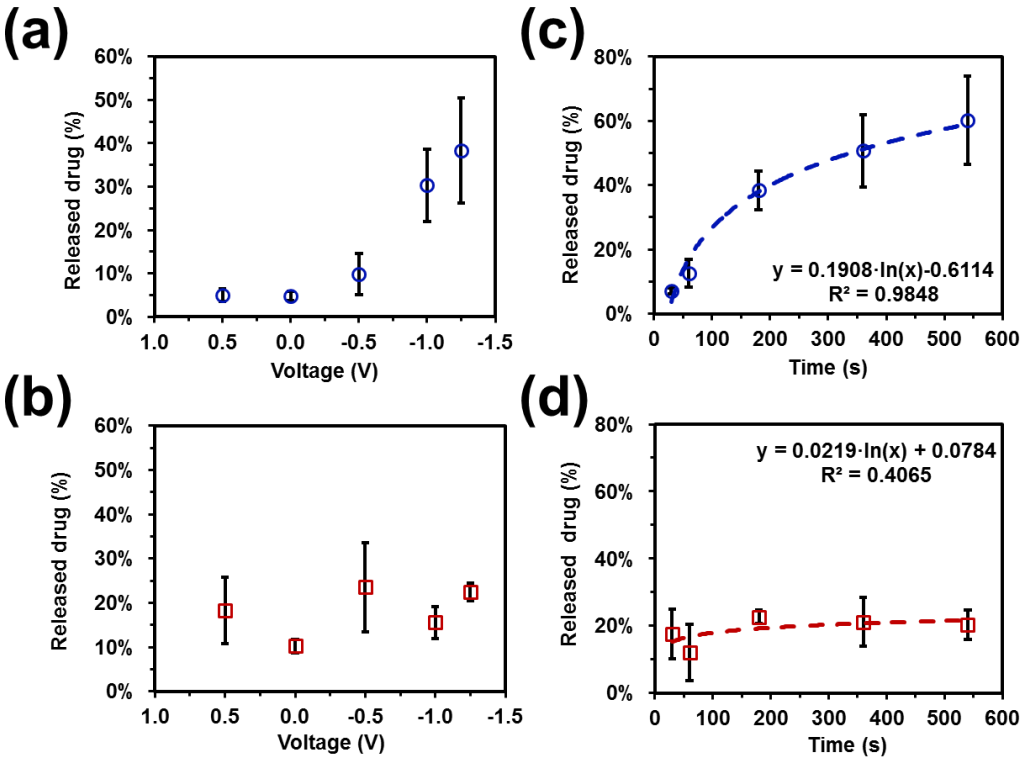
(a)
Released drug (%)
60%
50%
40%
30%
20%
10%
0%
1.0
0.5
0.0
-0.5
-1.0
-1.5
Voltage (V)
(c)
Released drug (%)
80%
60%
40%
20%
0%
y = 0.1908·ln(x)-0.6114
R² = 0.9848
0
100
200
300
400
500
600
Time (s)
(b)
Released drug (%)
60%
50%
40%
30%
20%
10%
0%
1.0
0.5
0.0
-0.5
-1.0
-1.5
Voltage (V)
(d)
Released drug (%)
80%
60%
40%
20%
0%
y = 0.0219·ln(x) + 0.0784
R² = 0.4065
0
100
200
300
400
500
600
Time (s)

Figure 7

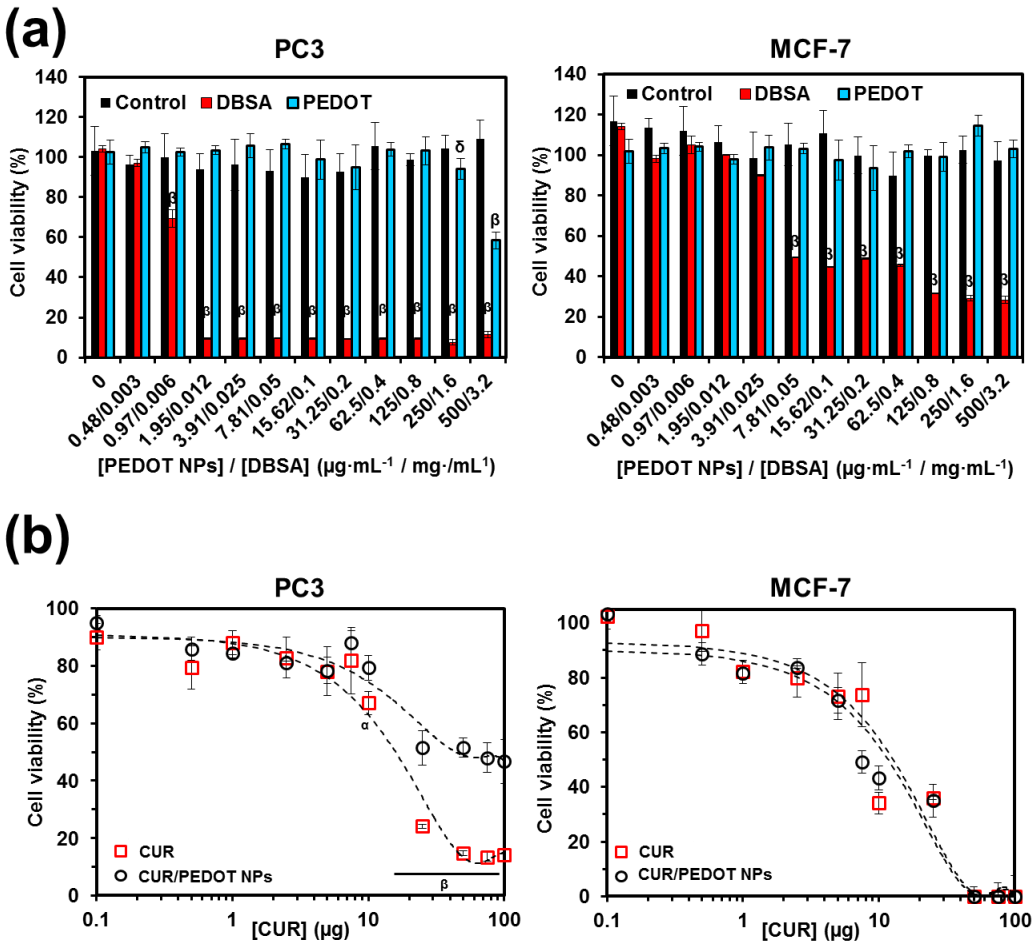
(a)
PC3
MCF-7
Control
DBSA
PEDOT
Cell viability (%)
[PEDOT NPs] / [DBSA] (μg·mL-1 / mg·mL-1)
0
0.48/0.003
0.97/0.006
1.95/0.012
3.91/0.025
7.81/0.05
15.62/0.1
31.25/0.2
62.5/0.4
125/0.8
250/1.6
500/3.2
(b)
PC3
MCF-7
CUR
CUR/PEDOT NPs
Cell viability (%)
[CUR] (μg)

Figure 8

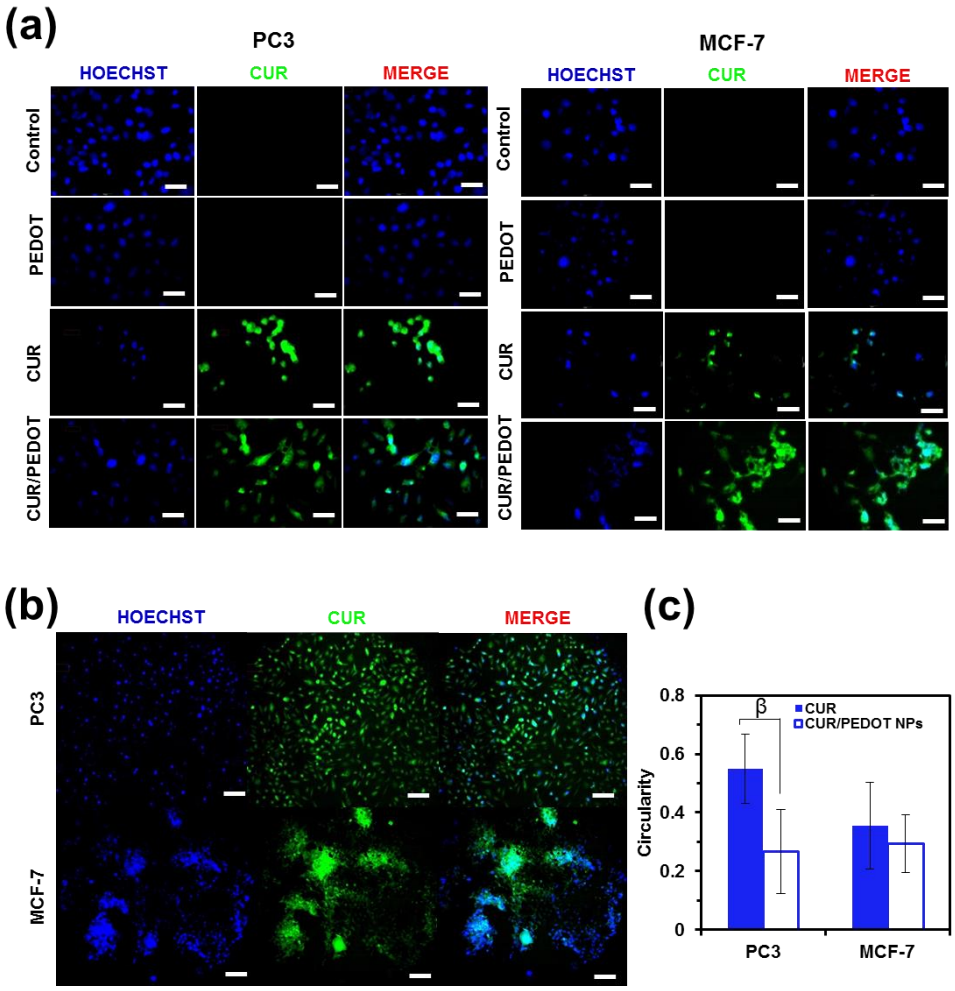
(a)
PC3
MCF-7
HOECHST
CUR
MERGE
Control
PEDOT
CUR
CUR/PEDOT
(b)
PC3
MCF-7
(c)
β
CUR
CUR/PEDOT NPs
Circularity
0.8
0.6
0.4
0.2
0
PC3
MCF-7

Figure 9

# TOC Graphic

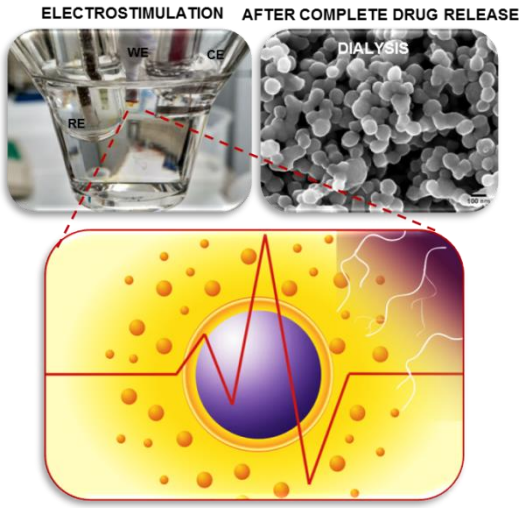


**Table of contents entry:**

**An electric field responsive polymeric nanoparticles system for programmed drug delivery is presented.** More specifically, curcumine loaded into stabilized poly(3,4-ethylenedioxythiophene) electroactive nanoparticles is released by applying a controlled external voltage. Curcumine···polymer interactions are crucial to regulate the release. This non-toxic biocompatible system is of potential use for advanced biomedical applications.